Received: 20 June 2019 | Revised: 27 September 2019 | Accepted: 1 October 2019

DOI: 10.1002/elsc.201900105

Engineering in Life Sciences

RESEARCH ARTICLE

# Thiol-ene photoclick reaction: An eco-friendly and facile approach for preparation of MPEG-g-keratin biomaterial

**Xianpan Ye | Jiugang Yuan | Zhe Jiang | Shuoxuan Wang | Ping Wang | Qiang Wang | Li Cui**

Key Laboratory of Eco-Textiles, Ministry of Education, Jiangnan University, Wuxi, P. R. China

**Correspondence**
Dr. Jiugang Yuan, Key Laboratory of Eco-Textiles, Ministry of Education, Jiangnan University, 1800 Lihu AVE, Wuxi 214122, P. R. China.
Email: jiugangyuan@163.com

Wool keratin is a natural material with excellent properties, which is considered as scaffold biomaterial for tissue engineering. Polyethylene glycol can improve the mechanical properties of keratin materials because of its excellent biocompatibility and plasticity. In the present work, poly (ethylene glycol) methyl ether methacrylate (MPEGMA) was grafted onto keratin by thiol-ene photoclick reaction. The results of FTIR and SDS-PAGE verified the successful reaction between MPEGMA and keratin. Compared with the keratin, circular dichroism and XRD results showed that the $\beta$-sheet ratio increased in MPEG-g-keratin. Additionally, it can be found that the exposure of keratin hydrophobic amino acids increased quickly and the micelle size became larger due to the introduction of MPEG from the results of fluorescence spectroscopy and particle size analysis. The MPEG-g- keratin was formed into a membrane to further study the application of the modified keratin. Compared with the keratin membrane, the flexibility and biocompatibility of modified keratin have been improved. This work provides an eco-friendly and facile approach for preparation of the keratin biomaterials.

**KEYWORDS**
biomaterial, keratin, MPEGMA, thiol-ene photoclick

## 1 | INTRODUCTION

Keratin is a renewable resource, which is widely distributed in wool, hair, feathers, hooves, and horns [1]. Wool has been estimated worldwide by-products from textile processing, hair and feathers from butchery more than 5 million tons per year [2,3]. Hence, various methods have been made to extract keratin from the wasted resources. Chemical methods mostly employ strong acids, alkali hydrolysis, and other chemicals containing peroxides, sulfites, dithiothreitol, and thiols [4]. Wool keratin, a kind of unbranched polymer comprised of amino acids, exhibits a stable 3-D conformation maintained by a range of non-covalent interactions and covalent interactions, in addition to the peptide bonds between individual amino acids [5]. Recent researches have reported that the regenerated keratin obtained by the reduction method has a unique Arg-Gly-Asp-Ser (RGDS) structure at its end, which makes its biocompatibility better than other biomaterials such as collagen and silk fibroin [6,7]. Warwick J. Duncan et al. implanted keratin hydrogel into the distal femoral condyle

Abbreviations: ANS, 8-anilino-1-naphthalenesulfonic acid ammonium salt; CD, circular dichroism; DLS, dynamic light scattering; HMPP, 2-hydroxy-2-methylpropiophenone; MPEGMA, poly (ethylene glycol) methyl ether methacrylate; PEG, polyethylene glycol; XRD, X-ray diffraction.

of sheep and found that keratin hydrogel has the potential to enhance successful osseointegration of dental implants placed in inferior bone [8]. Xiangyu Xu et al. found that the wool keratin adsorbed and stabilized $MoS_2$ nanosheets provided excellent biocompatibility in the cultivation of osteoblasts [9].

However, there is a brittle problem in pure regenerated keratin materials, which leads to difficulties in the formation of keratin membranes or fibers [10]. Thus, it is hard to meet the demand for tissue engineering materials which require high mechanical property. Fortunately, the keratin side chain contains a large number of amino, carboxyl, sulfhydryl, and hydroxyl groups, which can be used as sites for photocatalytic grafting reactions [10,11]. Among them, the sulfhydryl group has the highest reactivity, which participates in the formation of disulfide bonds to confer keratin stability [12]. In addition, the disulfide bonds can be easily cleaved by reducing agents to form more thiols, which offer great opportunities for keratin to be modified and functionalized through the thiol-ene reaction [13–15]. There are many kinds of initiation mechanisms to initiate thiol-ene click reaction, such as thermal, photo and redox, in which photo initiation becomes more and more popular because of its high efficiency, versatility, and simplicity for the preparation of new functional polymer materials [16–20]. Chien-Chi Lin et al. fabricated polyethylene glycol (PEG) hydrogels through thiol-ene photoclick reaction for in situ cell encapsulation [21]. Yu, Bing et al. prepared thiol-ene photocrosslinked hybrid vesicles, which can be used to control the dispersion of both hydrophilic and hydrophobic dyes in water [22].

PEG, a linear or branched neutral polyether with a variety of molecular weights, is a very good choice to improve mechanical properties of keratin membrane [23]. Despite its apparent simplicity, it has been extensively studied because of its biocompatibility, non-toxicity, and low immunogenicity [24]. In addition, it is easy to be chemically modified and attach to other molecules and surfaces. When PEG is combined with other molecules, there is little effect on their chemical properties but controls their solubility and increases their size [23]. Therefore, PEGylation is becoming more and more popular for enhancing the biotechnological potential of keratin. Many researchers have reported that PEG has excellent plasticizing abilities [25,26], which can reduce keratin chain-to-chain interaction and increase membrane flexibility.

In the present work, we demonstrated a facile approach for grafting poly (ethylene glycol) methyl ether methacrylate (MPEGMA) onto wool keratin. The disulfide bonds in the keratin were reduced to thiol groups and then the thiol groups reacted with MPEGMA through thiol-ene photoclick reaction (Scheme 1). After the modification, the keratin membrane can be successfully prepared with better flexibility and biocompatibility, which shows a good inspiration for the modification of keratin biomaterials.

**PRACTICAL APPLICATION**

Wool keratin is known as a renewable resource around the world usable as potential sources for polyamides and also as a promising natural material for tissue engineering. Therefore, it is highly desirable to solve the brittleness problem of pure regenerative keratin materials. In this paper, MPEG soft segments were introduced onto keratin through thiol-ene photoclick reaction. The modified membrane is non-toxic without the introduction of metal ions. Meanwhile, the modified keratin membrane combines the advantages of keratin and MPEG with excellent biocompatibility and flexibility compared with the untreated keratin material. The method that is presented in this publication is eco-friendly and facile for preparation of the keratin biomaterial

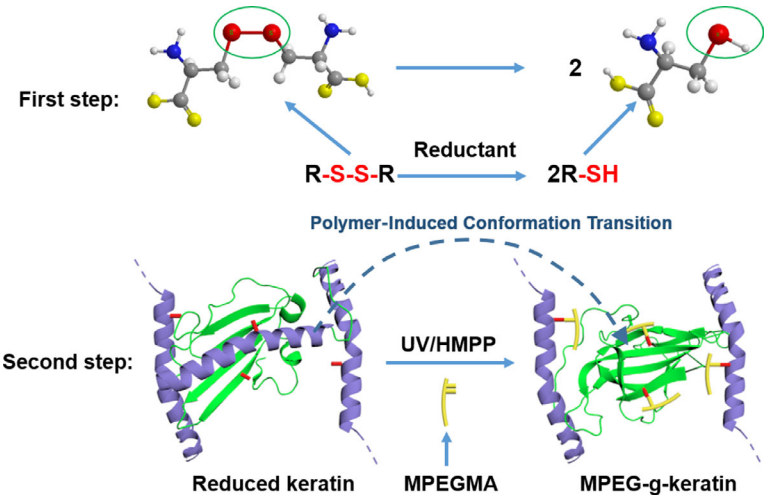


**SCHEME 1** Synthetic scheme for the preparation of MPEG-g-keratin

## 2 | MATERIALS AND METHODS

### 2.1 | Materials

Wool fiber was provided by Xiexin Worsted Spinning Weaving and Dyeing (Wuxi, China). MPEGMA (Mn = 300) was purchased from Sigma-Aldrich (Shanghai, China). 2-Mercaptoethanol was provided by Xiya reagent (Shandong, China). Tris (2-carboxyethyl) phosphine hydrochloride, 2-Hydroxy-2-methylpropiophenone (HMPP) and 8-anilino-1-naphthalenesulfonic acid ammonium salt (ANS) were purchased from Aladdin Reagent (Shanghai, China). All the other reagents used in this study were commercially available and were of analytical grade throughout.

### 2.2 | Extraction of wool keratin

Keratin was extracted from wool according to the method reported previously [27]. Wool fiber was cleaned by acetone in a Soxhlet extractor for 48 h. The degreased wool fiber (1 g) was dissolved in a solution (18 mL) containing 8 M urea, 0.5 M 2-mercaptoethanol, 0.1 M SDS, and the pH was adjusted to 9.5 with concentrated sodium hydroxide. The system was shaken in a water bath at 90°C for 6 h. After removing part of the insoluble deposits by vacuum filtration, the keratin solution was dialyzed against deionized water to remove the residual salts and urea. The sample solution was obtained after removal of insoluble precipitate again by centrifugation. Finally, keratin powder was obtained by keeping the sample solution at −20°C for 8 h, followed by freeze drying at −50°C for 48 h.

### 2.3 | Grafting procedure

The wool keratin (25 g/L) was dissolved in 8 M urea solution, and then the dissolved keratin was reduced with tris (2-carboxyethyl) phosphine hydrochloride (6 g/L) at 70°C. After 1 h, HMPP (2.5 mg/L) and MPEGMA (25 g/L) were added to the solution, subsequently exposed to 254 nm UV light (band width ≤5 nm, intensity = 5 mW) for 15 min. After the reaction, the mixture solution was dialyzed for 72 h to remove unreacted MPEGMA, urea and other impurities. Furthermore, adding only MPEGMA without HMPP (control sample) as a control was also performed under the same condition.

### 2.4 | Preparation of keratin membrane

Keratin solution (60 g/L) was first prepared. After thoroughly mixing with 0.5% w/v of glycerol, the solution was poured into a Teflon plate and naturally air-dried at 20°C and a relative humidity of 62%.

### 2.5 | Determination of free thiol (-SH) content

The free thiol content was measured according to literature procedures [28]. Fifteen milligrams of samples were placed in 0.8 mL buffer A (8 M urea, 3 mM EDTA, 1% SDS, and 0.2 M Tris-HCl, pH 8.0). Subsequently, the samples were shaken at room temperature for 2.5 h. And then, added 0.2 mL of Buffer B (50 mM DTNB reagent, 0.2 M Tris-HCl, pH 8.0). The samples were again shaken for 1 h, and the absorbance was measured at 412 nm. The blank control was buffer A (0.8 mL) and buffer B (0.2 mL). The free thiol content was calculated according to the molarextinction coefficient 13 600 L/(mol × cm).

### 2.6 | FTIR analysis

FTIR analysis was performed using a Nicolet iS10 spectrometer (Thermo, Nicolet, USA), and spectrum was recorded in the wavelength range 4000–500 $cm^{-1}$, at a resolution of 4 $cm^{-1}$ and 32 scans per sample.

### 2.7 | SDS-PAGE

According to the method of Pascal Bailon [29], the sample was subjected to SDS/polyacrylamide (8–16%) gel electrophoresis, and the keratin was stained with Coomassie blue dye.

The PEG part of the sample was specifically stained with barium iodide solution according to the method of literature [30]. The SDS-PAGE gel was rinsed with distilled water and placed in a 5% barium chloride solution. After 15 min, the gel was washed with distilled water and placed in a 0.1 M iodine solution for another 5 min. Iodine was washed off with distilled water.

### 2.8 | Particle size analysis

Particle size and its distribution for each keratin solution were determined at 25°C by dynamic light scattering (DLS), using a Malvern Zeta sizer Nano ZS90 instrument (Malvern, British) with a fixed angle of 90° [31]. The cumulate analysis was used for analyzing the DLS data of the different keratin samples.

### 2.9 | Circular dichroism test

Circular dichroism measurements of the keratin solution were performed using a MOS-450 Circular Dichroism instrument (Biologic, France), at a scanning rate of 100 nm/min from 190 to 250 nm. The samples were tested in a 1 mm quartz cuvette at 25°C.

## 2.10 | Fluorescence spectroscopy

Fluorescence spectroscopy was used to determine the degree of exposure of the hydrophobic amino acids of the keratin, and the solubility of the sample was diluted to 0.1 mg/mL with a phosphate buffer solution (pH = 7.4, 0.01 M). Sample containing 4 mL of solution was added 20 μL of ANS (8 mM) solution [32]. Then, the sample was tested in an F-4600 fluorescence spectrophotometer (Hitachi, Japan) with an excitation wavelength of 380 nm, a voltage of 800 V, and a slit width of 5 nm. The fluorescence intensity of the sample at the emission wavelength of 400–600 nm was measured.

## 2.11 | X-ray diffraction

X-ray diffraction (XRD) was performed using a Bruker D8 Focus with Cu target at 40 kV, 40 mA in the scanning range of 5–50° with a step size of 0.02°. The sample was evenly applied to the wafer surface when the test was conducted.

## 2.12 | Biocompatibility

The biocompatibility of keratin samples were tested by ISO 10993-5-2009 using NIH/3T3 cells [33]. After being sterilized by ethanol (75%) for 24 h, the samples were prepared using DMEM (containing 10% fetal bovine serum, 100 U/Ml penicillin and 100 μg/mL streptomycin) with a concentration of 5 mg/mL. 100 μL of the NIH/3T3 cell suspension and 50 μL of the sample were injected into the cell culture plate and diluted to 500 μL. Subsequently, the cell plate was kept at 37°C in a humidified atmosphere of 5% $CO_2$ for 48 h. Then, 10 μL CCK-8 solution was added and incubated for another 2 h. The absorbance at 450 nm was recorded by using an ELISA microplate readermicroplate reader. The viable cell percentage was calculated according to Eq. (1).

$$\textit{Viable cell percentage}\ (\%) = \frac{A_1}{A_0} \times 100 \qquad (1)$$

where, $A_1$ and $A_0$ are the absorbances for the sample and the blank, respectively.

# 3 | RESULTS AND DISCUSSION

## 3.1 | Determination of free thiol content

The degree of thiol reaction can be directly visualized by detecting the free thiol content of the sample. It can be seen from Figure 1 that the thiol group content of the control sample without adding photoinitiator (HMPP) was almost the same as that of keratin while the thiol group content of MPEG-g-keratin sample decreased dramatically. The result of free thiol content indicated that MPEGMA was successfully grafted onto keratin via thiol-ene click reaction.

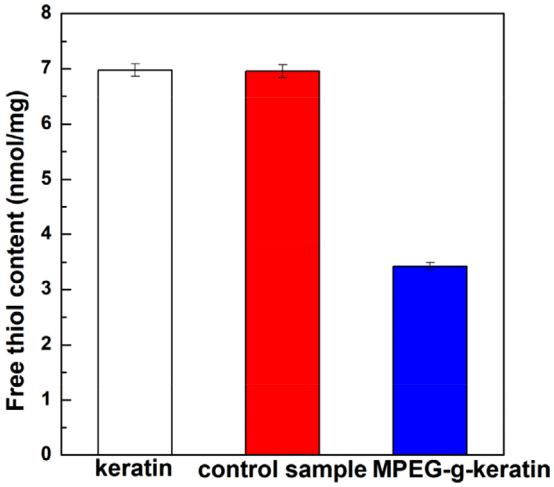


**FIGURE 1** Free thiol content of keratin and MPEG-g-keratin

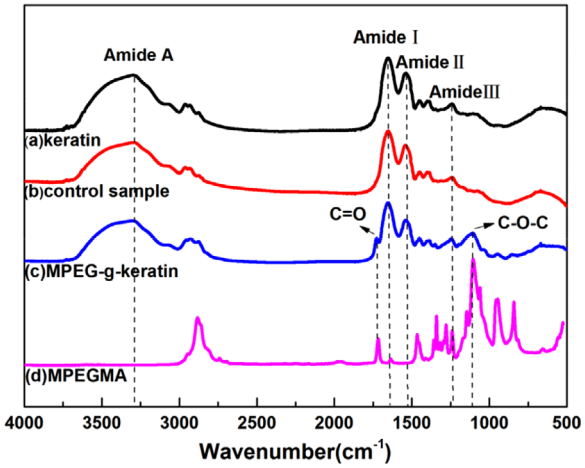


**FIGURE 2** FTIR spectra of keratin and MPEG-g-keratin

## 3.2 | Characterization of the keratin and MPEG-g-keratin

### 3.2.1 | FTIR spectroscopy

The FTIR spectra of keratin and MPEG-g-keratin were compared in Figure 2. The spectra contained characteristic peaks of peptide bonds (–CONH), and these characteristic peaks were classified into Amide A, Amide I, Amide II, and Amide III bands. An absorption peak at 3297 $cm^{-1}$ was assigned to N–H stretching (Amide A). A strong absorption peak at 1655 $cm^{-1}$ should be ascribed to the C=O (Amide I). A medium strong peak was observed at 1542 $cm^{-1}$ and assigned to C–N stretching and N–H in-plane bending vibrations (Amide II), while the weak band in the range of 1242 $cm^{-1}$ was related to the C–N and C–O stretching vibrations (Amide III) [1]. As for the spectra of the MPEGMA, a strong band at 1105 $cm^{-1}$ was ascribed to the C–O–C ether stretch and a band at 1716 $cm^{-1}$ assigned to the C=O stretch [34,35]. In Figure 2b, no additional bands were seen

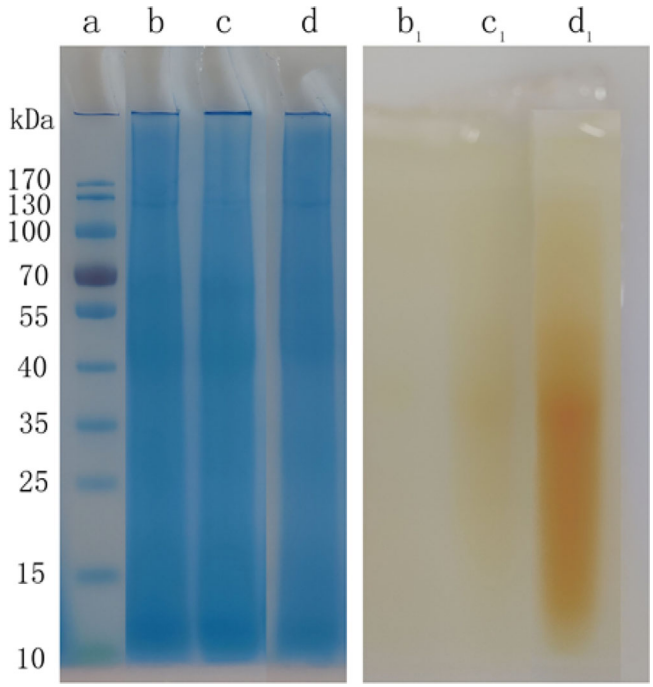


**FIGURE 3** SDS-PAGE of keratin and MPEG-g-keratin (a: protein standard, b: keratin, c: control sample, d: MPEG-g-keratin; $b_1$: keratin, $c_1$: control sample, $d_1$: MPEG-g-keratin)

in the control sample spectra, which meant that most of the unreacted MPEMGA was removed by dialysis. As for Figure 2c, two characteristic absorption peaks of MPEGMA at 1729 and 1105 $cm^{-1}$ can be observed, which confirmed the successful grafting of MPEGMA onto wool keratin via thiol-ene click reaction.

### 3.2.2 | SDS-PAGE

Figure 3 showed SDS-PAGE results of keratin (b), control sample (c), and MPEG-g-keratin (d). The three samples had a similar molecular weight distribution and mainly ranged between 40–70 kDa. This was mainly due to the small molecular weight of MPEGMA, which had little effect on the molecular weight of the grafted product. The results of PEG staining were shown in Figure 3 (b1, c1, and d1). The keratin (b1) was almost white after stained with barium iodide, because the sample does not contain MPEG and cannot react with barium iodide. While the control sample (c1) had a very light yellowish color maybe due to the small amount of MPEGMA adsorbed on the keratin by hydrogen bonding. The color of MPEG-g-keratin (d1) was deep yellow indicating that a large amount of MPEG was grafted onto keratin [30].

### 3.2.3 | Particle size

After the MPEG chains were grafted onto keratin, stronger hydrogen bonds were found between MPEG and keratin to shape a core-shell structure. Hydrophobic segments were segregated from the aqueous exterior to form an inner core

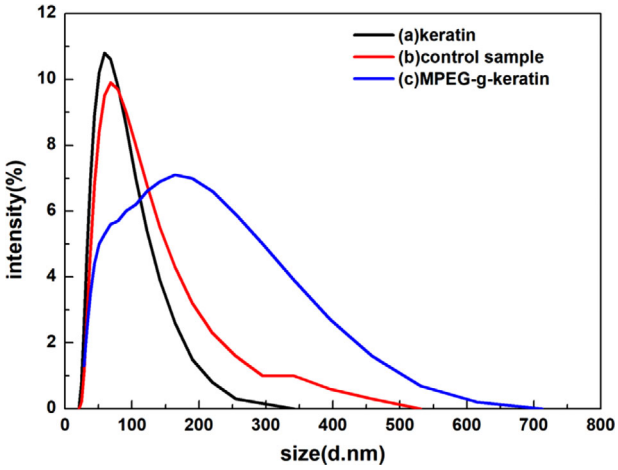


**FIGURE 4** Particle size and its distributions of keratin and MPEG-g-keratin

surrounded by a shell of hydrophilic segments, and thus formed micelles in the aqueous solution [36]. The diffusion coefficient of these micelles can be measured by DLS [37].

The particle sizes and polydispersity index (PDI) of the keratin was identified and shown in Figure 4. As can be seen, the average particle size of keratin was found to be 63.7 dnm with the PDI of 0.235. The control sample had an average particle size of 75.66 dnm with the PDI of 0.276, since some of the MPEGMA in the control sample was covalently bonded and adsorbed on the keratin peptide chain, so the average particle size was slightly increased. As for MPEG-g-keratin solution, the average particle size was 97.7 dnm with the PDI of 0.388 due to the increase of the hydrophilic MPEG chains. Meanwhile, the high PDI values can be attributed to higher MPEG content in keratin that could reduce the interactions of hydrophobic chains and create a steric barrier around keratin [38]. By introducing hydrophilic MPEG chains, the hydrophilicity of keratin can be increased, and the stability of keratin micelle in aqueous solution can be improved [39].

### 3.2.4 | Circular dichroism

The secondary structure of the keratin peptide chain follows the electronic transition caused by the peptide bond (–CONH–) and the modification induced by its supramolecular arrangement. Therefore, the changes in their photoconformation can be detected by circular dichroism (CD) spectroscopy [40].

The results of CD were shown in Figure 5. The $\alpha$-helical peptides presented a characteristic positive band at 193 nm and two negative bands at 208 and 222 nm [40]. The curve trends of the three samples were consistent, indicating that the secondary conformation of the sample was not greatly affected by the introduction of MPEG. However, the proportion of the secondary conformation had changed as shown in Table 1, which was calculated from their CD spectra. The

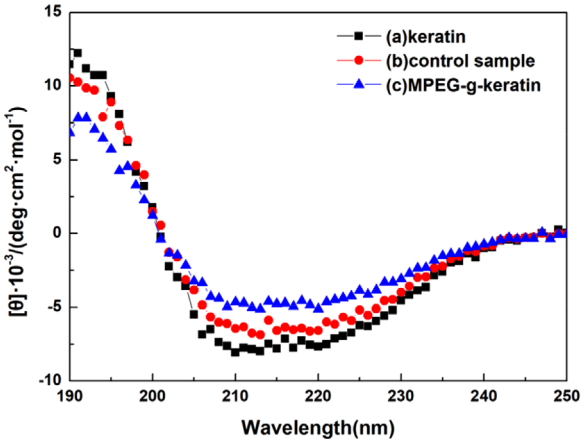


**FIGURE 5** CD of keratin and MPEG-g-keratin

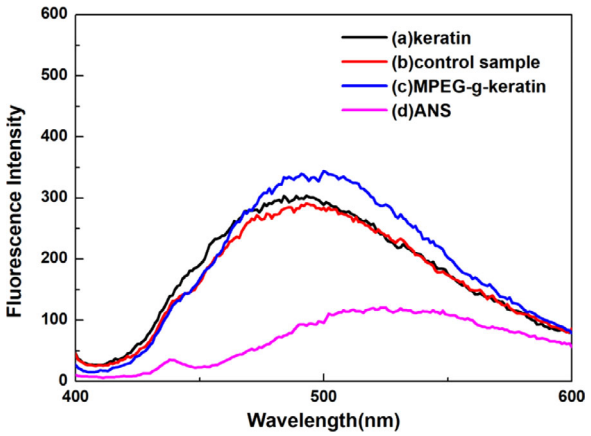


**FIGURE 6** Fluorescence spectroscopy of keratin and MPEG-g-keratin

**TABLE 1** Secondary structure content of keratin and MPEG-g-keratin

| Sample | α-helix% | β-sheet% | β-turn% | Random coil% |
|---|---|---|---|---|
| Keratin | 60.58 | 6.32 | 11.66 | 21.44 |
| Control sample | 54.21 | 8.71 | 13.41 | 23.68 |
| MPEG-g-keratin | 40.94 | 14.27 | 19.19 | 25.60 |

sample of keratin has the highest ratio of $\alpha$-helical structure and lowest ratio of $\beta$-sheet structure, while the sample of MPEG-g-keratin has the lowest ratio of $\alpha$-helical structure and lowest ratio of $\beta$-sheet structure. For the sample of MPEG-g-keratin, the ratio of $\beta$-sheet, $\beta$-turn, and random coil structure increased greatly, which was due to the keratin chain as a mold plate to stretch itself to form a $\beta$-sheet structure according to the strong hydrogen bond between MPEG and keratin. This conformational change was the "Polymer-Induced Conformation Transition" proposed by Xin Chen [41]. The $\beta$-sheet, $\beta$-turn and random coil ratios of the control sample increased slightly due to the introduction and removal of MPEGMA. MPEGMA can form stronger hydrogen bonds with amino acids of keratin, causing the peptide chain to stretch, which reduced the $\alpha$-helix ratio and promoted the formation of other secondary structures. This effect was preserved even if MPEGMA was dialyzed away.

### 3.2.5 | Fluorescence Spectroscopy

There are both hydrophilic amino acids and hydrophobic amino acids in the structure of keratin, and itself can constitute a biological macromolecule having a spatial structure with a hydrophobic amino acid as a core and a hydrophilic amino acid as a periphery [42]. Any change will affect the stability of keratin in aqueous solution. In order to study the effect of the introduction of MPEG on the hydrophobicity of keratin, the fluorescent probe method was used to analyze some

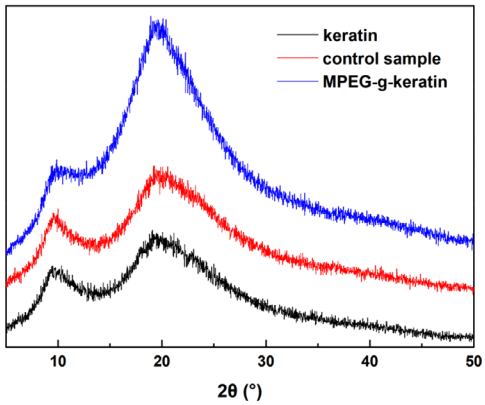


**FIGURE 7** XRD patterns of keratin and MPEG-g-keratin

hydrophobic amino acid residues contained in keratin, such as phenylalanine, tryptophan and tyrosine [43]. The change in fluorescence emission intensity can be used to analyze the effect of MPEGMA modification on the exposure of keratin hydrophobic amino acids.

As was shown in Figure 6, the fluorescence intensity of pure ANS at 530 nm was very weak. When the keratin was combined with ANS, a significant fluorescence peak appeared at 500 nm, indicating that some of the hydrophobic amino acids of keratin were exposed outside the peptide chain. However, the fluorescence emission intensity of the control sample was slightly lower than that of keratin, which may be due to that the steric hindrance of MPEGMA adsorbed on the keratin hindered the binding of the hydrophobic amino acid to the ANS. The fluorescence emission intensity of MPEG-g-keratin was higher than that of keratin, which indicated that the degree of exposure of hydrophobic amino acids was increased. The reason for this phenomenon was that the keratin was more hydrophilic after being grafted by MPEGMA, which caused the peptide chain to stretch and increased the exposure of hydrophobic amino acids.

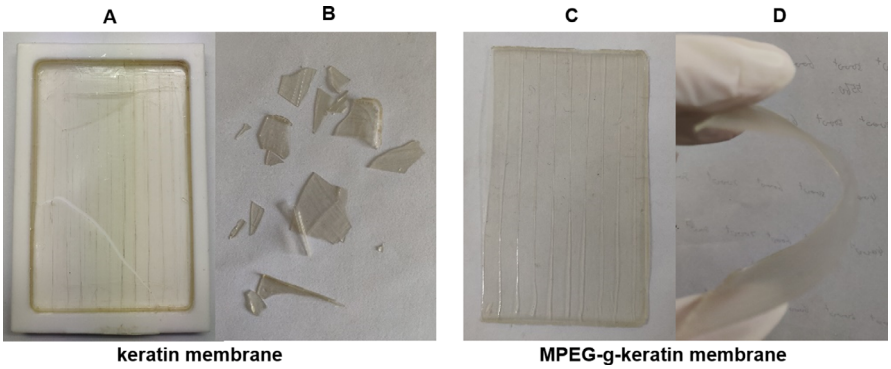


**FIGURE 8** The membrane of keratin and MPEG-g-keratin. (A) The keratin membrane after air-dried. (B) The keratin membrane after being squeezed. (C) The MPEG-g-keratin membrane after air-dried. (D) The MPEG-g-keratin after being squeezed)

## 3.3 | XRD

The XRD spectra of the keratin, control sample and MPEG-g-keratin were shown in Figure 7, all of these samples had two distinct peaks [44]. The $\alpha$-helix structure generally appeared at $2\theta = 9°$ and 17.8° and the $\beta$-sheet structure peaks appeared at $2\theta = 9°$ and 19°. However, due to the overlapping signals from the $\alpha$-helix and the $\beta$-sheet at about $2\theta = 17.8°$ and 19°, both peaks cannot be clearly assigned. The peaks of the MPEG-g-keratin at $2\theta = 9°$ and 19° was stronger than that of keratin, indicating an increase in the number of the $\beta$-sheet structure. While the peaks of the control sample $2\theta =$ at 9° and 19° only increases a little bit, which was in consistence with the result of CD.

## 3.4 | Properties of the keratin and MPEG-g-keratin membrane

The air-dried keratin membrane was shown in Figure 8. The keratin membrane (A and B) had been broken due to brittleness of the material when it was air-dried. While the membrane of MPEG-g-keratin (C and D) had a high toughness in the peptide chain segment, due to the introduction of MPEGMA, the forming property of membrane was improved. Biocompatibility of the keratin membrane was investigated using NIH/3T3 cell viability assay. As shown in Figure 9, cell viability of the keratin membrane was 96.2%, indicating that the material was non-cytotoxic and allowed cell attachment and proliferation. The cell viability of the MPEG-g-keratin membrane increased to 107.5%, which indicated that the keratin was not only non-toxic, but also had a proliferative effect on cells after grafted with MPEGMA. The testing data further proved that grafting of MPEGMA would help the improvement of the biocompatibility activity of keratin.

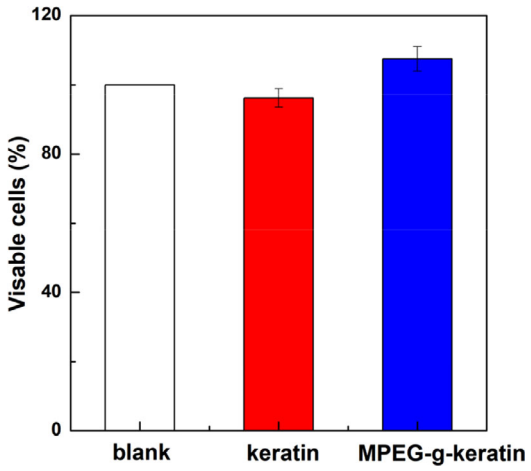


**FIGURE 9** Biocompatibility of keratin and MPEG-g-keratin

## 4 | CONCLUDING REMARKS

MPEG was grafted onto keratin through thiol-ene photoclick reaction and modified keratin membrane can be successfully prepared without any reduction in biocompatibility. The flexibility of the modified keratin was improved because MPEG has the effect of "Polymer- Induced Conformation Transition". The interaction between keratin and molecular chain-to-chain was waked, and PEG played a plasticizing role. As a result, the introduction of MPEG can induce the conformation of keratin chains and promote the formation of $\beta$-sheet. The combined effect of these factors improved the flexibility of membrane. It provided an effective way for producing keratin biomaterials. However, 2-mercaptoethanol and UV light employed in the paper are not eco-friendly, though the efficiency is relatively high. In the future, alternative methods such as L-cysteine and visible light can be employed to achieve a greener process.

## ACKNOWLEDGMENTS

This work was financially supported by the National Natural Science Foundation of China (31771039, 31300785, 51673087), Fundamental Research Funds for the Central Universities (JUSRP51717A), the National Key R&D Program of China (2017YFB0309200), the Open Project Program of Key

Laboratory of Eco-textiles, Ministry of Education, Jiangnan University (No.·KLET1504).

## CONFLICT OF INTEREST

The authors have declared no conflict of interest.

## REFERENCES


1. Wang, K., Li, R., Ma, J., Jian, Y., Che, J., Extracting keratin from wool by using L-cysteine. *Green Chem.* 2016, *18*, 476–481.
2. Zoccola, M., Aluigi, A., Tonin, C., Characterisation of keratin biomass from butchery and wool industry wastes. *J. Mol. Struct.* 2009, *938*, 35–40.
3. Eslahi, N., Dadashian, F., Nejad, N. H., An investigation on keratin extraction from wool and feather waste by enzymatic hydrolysis. *Prep. Biochem. Biotech.* 2013, *43*, 624–648.
4. Idris, A., Vijayaraghavan, R., Rana, U. A., Fredericks, D. et al., Dissolution of feather keratin in ionic liquids. *Green Chem.* 2013, *15*, 525–534.
5. Xie, H., Li, S., Zhang, S., Ionic liquids as novel solvents for the dissolution and blending of wool keratin fibers. *Green Chem.* 2005, *7*, 606–608.
6. Yamauchi, K., Hojo, H., Yamamoto, Y., Tanabe, T., Enhanced cell adhesion on RGDS-carrying keratin film. *Mat. Sci. Eng. C-Mater.* 2003, *23*, 467–472.
7. Andreia, V., Artur, C. P., The use of keratin in biomedical applications. *Curr. Drug Targets* 2013, *14*, 612–619.
8. Duncan, W. J., Greer, P. F. C., Lee, M.-H., Loch, C., Gay, J. H. A., Wool-derived keratin hydrogel enhances implant osseointegration in cancellous bone. *J. Biomed. Mater. Res. B* 2018, *106*, 2447–2454.
9. Xu, X., Wu, J., Meng, Z., Li, Y. et al., Enhanced exfoliation of biocompatible $MoS_2$ nanosheets by wool keratin. *ACS Appl. Nano Mater.* 2018, *1*, 5460–5469.
10. Sarac, A. S., Redox polymerization. *Prog. Polym. Sci.* 1999, *24*, 1149–1204.
11. Tsukada, M., Shiozaki, H., Freddi, G., Crighton, J. S., Graft copolymerization of benzyl methacrylate onto wool fibers. *J. Appl. Polym. Sci.* 1997, *64*, 343–350.
12. Tachibana, A., Furuta, Y. H., Tanabe, T., Yamauchi, K., Fabrication of wool keratin sponge scaffolds for long-term cell cultivation. *J. Biotechnol.* 2002, *93*, 165–170.
13. Yu, D., Cai, J. Y., Church, J. S., Wang, L., Modifying surface resistivity and liquid moisture management property of keratin fibers through thiol–ene click reactions. *Acs Appl. Mater. Inter.* 2014, *6*, 1236–1242.
14. Liu, P., O'mara, B. W., Warrack, B. M., Wu, W. et al., A tris (2-carboxyethyl) phosphine (TCEP) related cleavage on cysteine-containing proteins. *J. Am. Soc. Mass Spectr.* 2010, *21*, 837–844.
15. Burns, J. A., Butler, J. C., Moran, J., Whitesides, G. M., Selective reduction of disulfides by tris (2-carboxyethyl) phosphine. *J. Org. Chem.* 1991, *22*, 2648–2650.
16. Garg, S. M., Xiong, X., Lu, C., Lavasanifar, A., Application of click chemistry in the preparation of poly(ethylene oxide)-block-poly($\varepsilon$-caprolactone) with hydrolyzable cross-links in the micellar core. *Macromolecules* 2011, *39*, 2058–2066.
17. Liu, Y., Hou, W., Sun, H., Cui, C. et al., Thiol–ene click chemistry: a biocompatible way for orthogonal bioconjugation of colloidal nanoparticles, *Chem. Sci.* 2017, *8*, 6182–6187.
18. Zhang, S., He, X., Chen, L., Zhang, Y., Boronic acid functionalized magnetic nanoparticles via thiol–ene click chemistry for selective enrichment of glycoproteins, *New J. Chem.* 2014, *38*, 4212–4218.
19. Wu, J. T., Huang, C. H., Liang, W. C., Wu, Y. L. et al., Reactive polymer coatings: a general route to thiol-ene and thiol-yne click reactions. *Macromol. Rapid Comm.* 2012, *33*, 922–927.
20. Wendeln, C., Rinnen, S., Schulz, C., Arlinghaus, H. F., Ravoo, B. J., Photochemical microcontant printing by thiol-ene and thiol -yne click chemistry. *Langmuir the Acs J. Surfaces & Colloids* 2010, *26*, 15966–15971.
21. Lin, C. C., Raza, A., Shih, H., PEG hydrogels formed by thiol-ene photo-click chemistry and their effect on the formation and recovery of insulin-secreting cell spheroids. *Biomaterials* 2011, *32*, 9685–9695.
22. Yu, B., Jiang, X., Qin, N., Jie, Y., Thiol–ene photocrosslinked hybrid vesicles from co-assembly of POSS and poly(ether amine) (PEA). *Chem. Commun.* 2011, *47*,12110-12112.
23. Harris, J. M., *Introduction to Biotechnical and Biomedical Applications of Poly(Ethylene Glycol)*, Springer, Boston, MA 1992.
24. Slavin, S., Khoshd, E., Haddleton, D. M., PEGylation of surface protein filaments: coverage and impact on denaturation. *RSC Adv.* 2011, *1*, 58–66.
25. Yu, Y., Yan, C., Ren, J., Cao, E. et al., Plasticizing effect of poly(ethylene glycol)s with different molecular weights in poly(lactic acid)/starch blends. *J. Appl. Polym. Sci.* 2015, *132*, 41808.
26. DomjáN, A., Bajdik, J. N., Pintye-HóDi, K. R., Understanding of the plasticizing effects of glycerol and PEG 400 on chitosan films using solid-state NMR spectroscopy. *Macromolecules* 2009, *42*, 4667–4673.
27. Yamauchi, K., Yamauchi, A., Kusunoki, T., Kohda, A., Konishi, Y., Preparation of stable aqueous solution of keratins, and physiochemical and biodegradational properties of films. *J. Biomed. Mater. Res. B* 1996, *31*, 439–444.
28. Chan, K. Y., Wasserman, B. P., Direct colorimetric assay of free thiol groups and disulfide bonds in suspensions of solubilized and particulate cereal proteins. *Cereal Chem.* 1993, *70*, 22–26.
29. Bailon, P., Palleroni, A., Schaffer, C. A., Spence, C. L. et al., Rational design of a potent, long-lasting form of interferon: a 40 kDa branched polyethylene glycol-conjugated interferon $\alpha$-2a for the treatment of hepatitis C. *Bioconjug. Chem.* 2001, *12*, 195–202.
30. Kurfürst, M. M., Detection and molecular weight determination of polyethylene glycol-modified hirudin by staining after sodium dodecyl sulfate-polyacrylamide gel electrophoresis. *Anal. Biochem.* 1992, *200*, 244–248.
31. Xu, Y., Liu, J., Du, C., Fu, S., Liu, X., Preparation of nanoscale carbon black dispersion using hyper-branched poly(styrene- alt -maleic anhydride). *Prog Org Coat.* 2012, *75*, 537–542.
32. Haskard, C. A., Li-Chan, E. C. Y., Hydrophobicity of bovine serum albumin and ovalbumin determined using uncharged (PRODAN) and anionic (ANS-) fluorescent probes. *J. Agr. Food Chem.* 1998, *46*, 2671–2677.
33. Zhou, Q., Cui, L., Ren, L., Wang, P. et al., Preparation of a multifunctional fibroin-based biomaterial via laccase-assisted grafting of chitooligosaccharide. *Int. J. Biol. Macromol.* 2018, *113*, 1062–1072.
34. Fan, Q.-L., Neoh, K.-G., Kang, E.-T., Shuter, B., Wang, S.-C., Solvent-free atom transfer radical polymerization for the

preparation of poly (poly (ethyleneglycol) monomethacrylate)-grafted $Fe_3O_4$ nanoparticles: synthesis, characterization and cellular uptake. *Biomaterials* 2007, *28*, 5426–5436.
35. Shi, Y., Liu, Z., Yang, Y., Xu, X. et al., Design of poly(mPEGMA-co -MAA) hydrogel-based mPEG-b-PCL nanoparticles for oral meloxicam delivery. *Mat. Sci. Eng. C-Mater.* 2017, *76*, 975–984.
36. Shi, Y., Sun, F., Dan, W., Zhang, R. et al., Enhancement of bioavailability by formulating rhEPO ionic complex with lysine into PEG–PLA micelle. *J. Nanopart. Res.* 2013, *15*, 1–10.
37. Takahashi, K., Kato, H., Kinugasa, S., Development of a standard method for nanoparticle sizing by using the angular dependence of dynamic light scattering. *Anal. Sci.* 2011, *27*, 751–756.
38. Zhao, J., Wang, H., Liu, J., Deng, L. et al., Comb-like amphiphilic copolymers bearing acetal-functionalized backbones with the ability of acid-triggered hydrophobic-to-hydrophilic transition as effective nanocarriers for intracellular release of curcumin, *Biomacromolecules* 2013, *14*, 3973–3984.
39. Logie, J., Owen, S. C., Mclaughlin, C. K., Shoichet, M. S., PEG-graft density controls polymeric nanoparticle micelle stability, *Chem. Mater.* 2014, *26*, 2847–2855.
40. Gattuso, H., García-Iriepa, C., Sampedro, D., Monari, A., Marazzi, M., Simulating the electronic circular dichroism spectra of photoreversible peptide conformations, *J. Chem. Theory Comput.* 2017, *13*, 3290–3296.
41. Xin, C., Li, W., Yu, T., Conformation transition of silk fibroin induced by blending chitosan, *J. Polym. Sci. Pol. Phys.* 1997, *35*, 2293–2296.
42. Meirovitch, H., Rackovsky, S., Scheraga, H. A., Empirical studies of hydrophobicity. 1. Effect of protein size on the hydrophobic behavior of amino acids, *Macromolecules* 1980, *13*, 1398–1405.
43. Alizadeh-Pasdar, N., Li-Chan, E. C., Comparison of protein surface hydrophobicity measured at various pH values using three different fluorescent probes, *J. Agr. Food Chem.* 2000, *48*, 328–334.
44. Jiang, Z., Yuan, J., Wang, P., Fan X. et al., Dissolution and regeneration of wool keratin in the deep eutectic solvent of choline chloride-urea, *Int. J. Biol. Macromol.* 2018, *119*, 423–430.

**How to cite this article:** Ye X, Yuan J, Jiang Z, et al. Thiol-ene photoclick reaction: An eco-friendly and facile approach for preparation of MPEG-g-keratin biomaterial. *Eng Life Sci*. 2020;20:17–25. https://doi.org/10.1002/elsc.201900105